JACC: BASIC TO TRANSLATIONAL SCIENCE
VOL. 1, NO. 7, 2016
ISSN 2452-302X
http://dx.doi.org/10.1016/j.jacbts.2016.08.008

PRECLINICAL RESEARCH

Adeno-Associated Virus Serotype 9–Driven Expression of BAG3 Improves Left Ventricular Function in Murine Hearts With Left Ventricular Dysfunction Secondary to a Myocardial Infarction

Tijana Knezevic, PhD,[a,b] Valerie D. Myers, MS,[c] Feifei Su, MD, PhD,[c,d] JuFang Wang, MD,[e] Jianliang Song, MD, PhD,[e] Xue-Qian Zhang, MD,[e] Erhe Gao, MD, PhD,[e] Guofeng Gao, MD, PhD,[c] Muniswamy Madesh, PhD,[e] Manish K. Gupta, PhD,[b] Jennifer Gordon, PhD,[b] Kristen N. Weiner, BS,[c] Joseph Rabinowitz, PhD,[e] Frederick V. Ramsey, PhD,[f] Douglas G. Tilley, PhD,[e] Kamel Khalili, PhD,[b] Joseph Y. Cheung, MD, PhD,[c,e] Arthur M. Feldman, MD, PhD[c]

VISUAL ABSTRACT

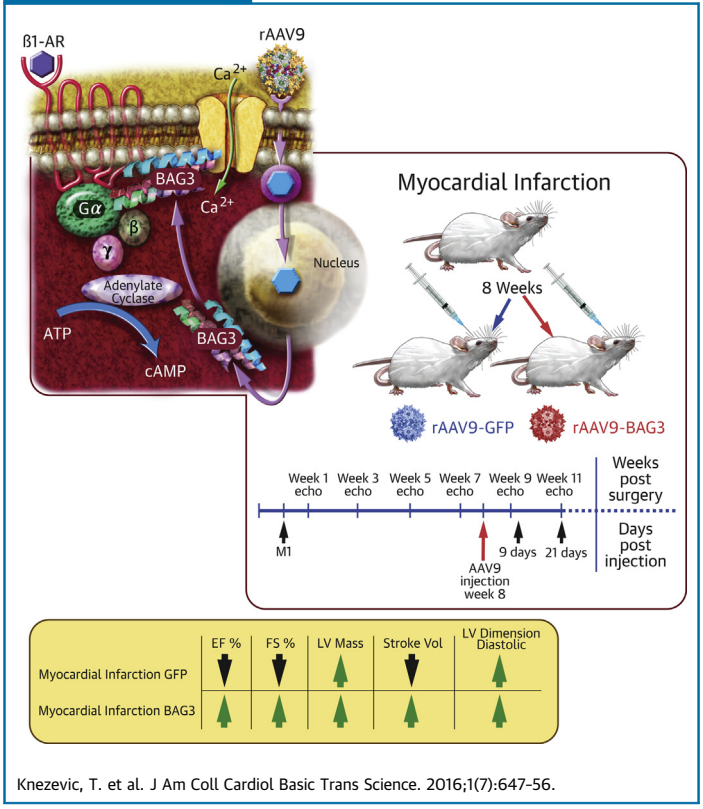

Knezevic, T. et al. J Am Coll Cardiol Basic Trans Science. 2016;1(7):647–56.

HIGHLIGHTS

- **BAG3 is a highly conserved protein having pleiotropic effects that is expressed at high levels in the heart, skeletal muscles, and many cancers.**
- **BAG3 levels are reduced in many forms of LV dysfunction including mice after ligation of the left coronary artery.**
- **Retro-orbital injection of mice with an adeno-associated virus coupled to murine BAG3 under the control of a CMV promoter (rAAV9-BAG3) increased myocardial levels of BAG3 by 7 days post-injection.**
- **Retro-orbital injection of rAAV9-BAG3 in mice post-myocardial infarction improved LV function, whereas rAAV9-BAG3 had no effect on LV function in the absence of an MI.**
- **BAG3 may prove to be a new therapeutic target in the treatment of heart failure.**

ABBREVIATIONS AND ACRONYMS

BAG3 = Bcl-2-associated athanogene 3

Bcl-2 = B-cell lymphoma 2

HF = heart failure

LV = left ventricular

LVEF = left ventricular ejection fraction

MI = myocardial infarction

rAAV9 = recombinant adeno-associated virus, serotype 9

SUMMARY

Mutations in Bcl-2-associated athanogene 3 (BAG3) were associated with skeletal muscle dysfunction and dilated cardiomyopathy. Retro-orbital injection of an adeno-associated virus serotype 9 expressing BAG3 (rAAV9-BAG3) significantly ($p < 0.0001$) improved left ventricular ejection fraction, fractional shortening, and stroke volume 9 days post-injection in mice with cardiac dysfunction secondary to a myocardial infarction. Furthermore, myocytes isolated from mice 3 weeks after injection showed improved cell shortening, enhanced systolic $[Ca^{2+}]_i$ and increased $[Ca^{2+}]_i$ transient amplitudes, and increased maximal L-type Ca^{2+} current amplitude. These results suggest that BAG3 gene therapy may provide a novel therapeutic option for the treatment of heart failure. (J Am Coll Cardiol Basic Trans Science 2016;1:647-56)

B-cell lymphoma 2 (Bcl-2)-associated anthanogene-3 (BAG3), a 575 amino acid member of the BAG family of proteins, is expressed at high levels in the heart, in the vasculature, and in many cancers (1). BAG3 plays an important role in protein quality control by serving as a co-chaperone for the heat shock proteins and attenuates apoptosis by binding to Bcl-2, which in turn leads to resistance to chemotherapy in cancer cells (2). In muscle, BAG3 also binds to capping protein (CapZ) to tether actin filaments to the Z-disc. That BAG3 plays a critical role in cardiac homeostasis was first shown by studies reporting that a heterozygous p.Pro209Leu mutation was associated with progressive limb and axial muscle weakness, severe respiratory insufficiency, and cardiomyopathy in children (3,4). Subsequent studies identified an association between deletions in BAG3 and the development of left ventricular (LV) dysfunction and cardiac dilation independent of peripheral muscle weakness in individuals with familial dilated cardiomyopathy (5,6). Decreased levels of BAG3 were also found in the ventricular myocardium of patients with end-stage heart failure (HF) and reduced ejection fraction due to either coronary artery disease or to idiopathic dilated cardiomyopathy (5).

Homozygous deletion of BAG3 in mice led to severe LV dysfunction, myofibril disorganization, and death by 4 weeks of age (7); however, the molecular mechanisms responsible for regulation of BAG3 function in the heart are just beginning to be understood. For

SEE PAGE 657

example, knock down of BAG3 in cultured neonatal mouse myocytes led to myofibrillar disarray, but only when the cells were stretched (8). By contrast, in adult murine myocytes, BAG3 localized at the sarcolemma and t-tubules where it modulated myocyte contraction and action potential duration through specific interaction with the β1-adrenergic receptor and L-type Ca^{2+} channels (9). BAG3 knockdown reduced contraction and $[Ca^{2+}]_i$ transient amplitudes in response to isoproterenol: changes that could be rescued by treatment with forskolin or dibutyryl cyclic adenosine monophosphate (9). These studies led us to hypothesize that enhanced expression of BAG3 could have salutary effects on myocardial function in hearts with diminished LV function. In this proof-of-concept study, we demonstrate for the first time that the administration of recombinant adeno-associated virus, serotype 9 (rAAV9)-BAG3 improves LV function in

From the [a]Department of Biology, College of Science and Technology, Temple University, Philadelphia, Pennsylvania; [b]Department of Neuroscience, Lewis Katz School of Medicine at Temple University, Philadelphia, Pennsylvania; [c]Department of Medicine, Lewis Katz School of Medicine at Temple University, Philadelphia, Pennsylvania; [d]Department of Cardiology, TangDu Hospital, Fourth Military Medical University, Xi'an, China; [e]Center for Translational Medicine, Lewis Katz School of Medicine at Temple University, Philadelphia, Pennsylvania; and the [f]Department of Clinical Sciences, Lewis Katz School of Medicine at Temple University, Philadelphia, Pennsylvania. This study was supported by grants from the National Institutes of Health Grant #P01 HL 091799-01 (to Dr. Feldman) and Grant #R01 HL123093 (to Drs. Khalili, Cheung, and Feldman). Ms. Myers and Drs. Tilley, Cheung, and Feldman have equity in Renovacor, Inc. Dr. Tilley has equity in Renovacor, Inc. Dr. Feldman is cofounder of and has equity in Renovacor, Inc. Drs. Tilley, Khalili, and Feldman have a pending U.S. patent: 61/934,483, BAG3 as a target for therapy of heart failure. Drs. Cheung and Feldman have a pending U.S. patent: 62/205,990, BAG3 composition and methods. Exclusive rights to the patents have been optioned by Temple University to Renovacor, Inc. All other authors have reported that they have no relationships relevant to the contents of this paper to disclose. Dr. Knezevic and Ms. Myers contributed equally to this work. Drs. Cheung and Feldman also contributed equally to this work.

Manuscript received June 7, 2016; revised manuscript received August 22, 2016, accepted August 25, 2016.

mice with LV dysfunction secondary to a myocardial infarction (MI). These studies suggest that BAG3 could be a novel target for therapeutic intervention in patients with HF with reduced ejection fraction.

METHODS

ANIMAL PROTOCOLS. Eight-week old male C57BL/6J mice (Jackson Laboratory, Bar Harbor, Maine) were randomly assigned to undergo an induction of an MI by left coronary artery ligation using a protocol described previously by our group that led to a significant reduction in LV function with generally acceptable levels of long-term survival (10,11). Consistent with earlier studies, nearly one-half of all infarcted mice expired within 1 week of surgery, but only 1 mouse died after week 1. Therefore, mice in which the artery was ligated were randomized to receive either gene therapy with BAG3 (rAAV9-BAG3; MI-BAG3, n = 13) or control (rAAV9-GFP; MI-GFP, n = 12) 1 week after surgery and prior to the first echocardiogram to obviate an effect of the early mortality in the model affecting outcomes. The mouse that died after week 1 had been randomized to MI-GFP and was not included in the analysis. Sham-operated control animals were treated in an identical manner except that the left anterior descending artery was not ligated. Sham mice were also randomized at the time of the week-1 echocardiogram to receive either BAG3 (rAAV9-BAG3; Sham-BAG3, n = 12) or a GFP control (rAAV9-GFP; Sham-GFP, n = 14). All experiments were performed according to the National Institutes of Health *Guide for the Care and Use of Laboratory Animals* and were approved by the Temple University Institutional Animal Care and Use Committee (ACUP#4360).

ECHOCARDIOGRAPHY. Global LV function was evaluated in all mice after light sedation (2% isoflurane) using a Vevo 770 imaging system and a 707 scan head (VisualSonics, Miami, Florida) as described previously (12). The first echocardiogram was obtained 1 week after surgery. The left ventricular ejection fraction (LVEF) was calculated using the formula EF% = ([LV end-diastolic volume - LV end-systolic volume]/LV end-diastolic volume) × 100. Fractional shortening (FS) was calculated as FS%= ([LV end-diastolic dimension − LV end-systolic dimension]/LV end-diastolic dimension) × 100.

CONSTRUCTION AND ADMINISTRATION OF rAAV9-BAG3. A sequence encoding the murine myc-tagged BAG3 (NCBI accession #BC145765) was inserted into a pAAV vector that contained a cytomegalovirus (CMV) promoter (Vector Biolabs, Malvern, Pennsylvania). The construct was then packaged into AAV-9 by transfection of HEK293 cells, and viral particles were purified by $CsCl_2$ centrifugation (Vector Biolabs). Recombinant AAV9-BAG3 also expressed green fluorescent protein (GFP); however, GFP was not in sequence with BAG3. Fidelity of the clone and the final vector were confirmed by sequencing. Both MI mice and Sham mice were randomly assigned to receive either 60 to 80 μl rAAV9-BAG3 (5.0 to 6.5 × 10^{13} genome copies (GC)/ml) or rAAV9-GFP control (3.1 × 10^{12} GC/ml) in sterile phosphate buffered saline (PBS) at 37°C by injection into the retro-orbital venous plexus as described previously (13).

IMMUNOBLOTS. Hearts were rapidly frozen in liquid nitrogen and stored at −80°C. Tissue was lysed in buffer (Cell Signaling Technologies, Beverly, Massachusetts) and homogenized with beads in a Bullet Blender (Next Advance, Averill Park, New York). After centrifugation at 13,000 *g* for 5 min at 4°C, the supernatant was collected and protein concentration was determined by Bradford assay (Bio-Rad, Philadelphia, Pennsylvania). Equal amounts of protein were mixed with 10 μl of 5× loading buffer (350 mmol/l Tris pH 6.8, 25% β-mercaptoethanol, 30% glycerol, 10% sodium dodecyl sulfate, and 0.01% bromophenol blue), boiled, separated on sodium dodecyl sulfate-polyacrylamide gel electrophoresis, and transferred to Odyssey nitrocellulose membranes (LiCor, Lincoln, Nebraska) by wet transfer (Bio-Rad). Membranes were blocked in Odyssey blocking buffer (LiCor) for 1 h at room temperature (rt) before incubation with primary antibodies for 2 h at rt. The membranes were then washed with 1× PBST (0.1% Tween 20 in PBS) and incubated with the secondary antibody for 1 h at rt. The signal was detected with an Odyssey scanner. Primary antibodies were Myc (Cell Signaling Technologies), BAG3 (ProteinTech Group Inc., Rosemont, Illinois), GFP (Clonetech, Mountain View, California), or glyceraldehyde-3-phosphate dehydrogenase (GAPDH) (Santa Cruz Biotechnology, Dallas, Texas) and calsequestrin (1:5,000) (Swant, Bellinzona, Switzerland). Calsequestrin was used to determine protein loading in quantitative Western blots, whereas GAPDH was used for nonquantitative blots. Secondary antibodies were: goat antimouse IRDye 800 (LiCor) and IRDye 680 goat antirabbit (Rockland, Gilbertsville, Pennsylvania).

ISOLATION OF ADULT MURINE CARDIAC MYOCYTES. In a subset of the study cohort, cardiac myocytes were isolated from the septum and LV free wall according to the protocol of Zhou et al. (14) and plated on laminin-coated glass coverslips (15). Coverslips containing myocytes were mounted in a Dvorak-Stotler chamber, and bathed in fresh media before measurements.

FIGURE 1 rAAV9-BAG3 Improves LV Function in Mice With LV Dysfunction Secondary to Ligation of the Left Coronary Artery

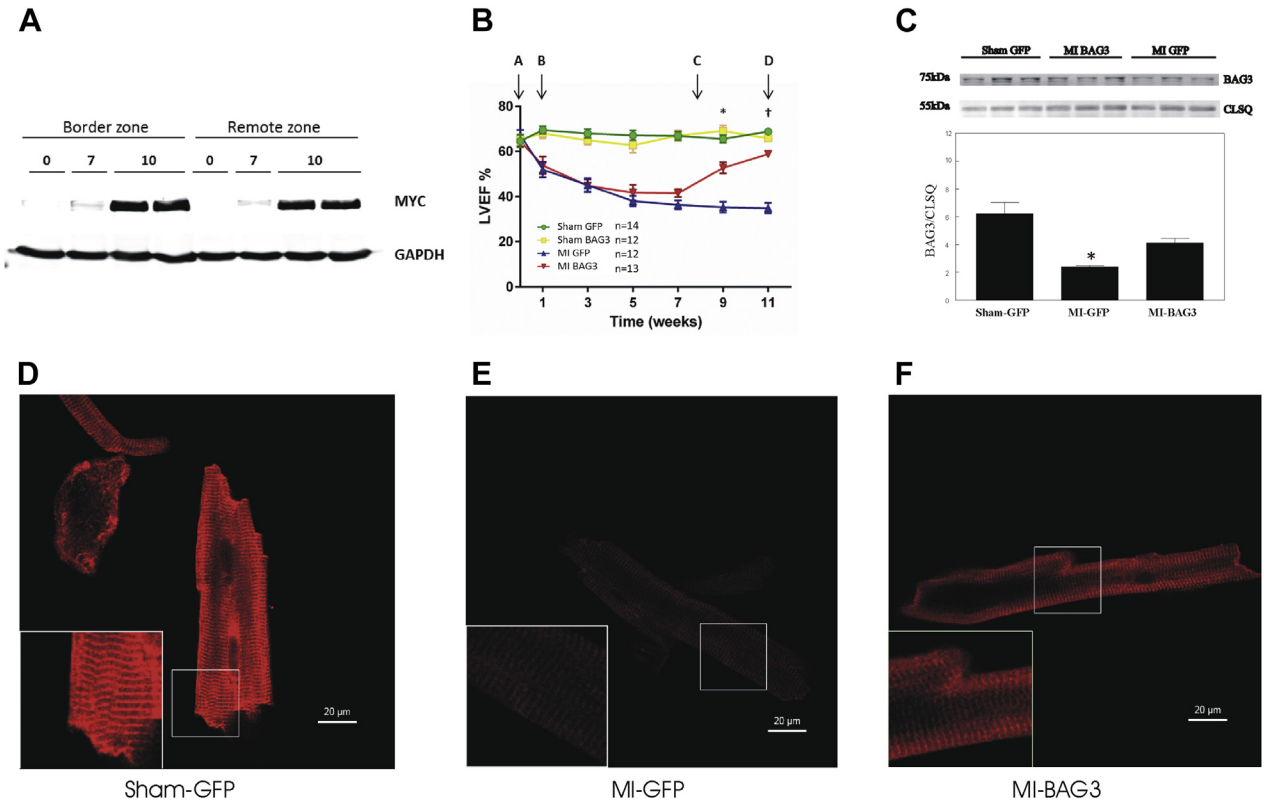

(A) Western blot analysis of tissue obtained on various days from mice after retro-orbital injection of myc^{-}-tagged adeno-associated virus serotype 9 expressing BAG3 (rAAV9-BAG3). **(B)** Eight-week-old C57BL/6J were subjected to ligation of the left coronary artery (myocardial infarction [MI]) or sham surgery (Sham) (week 0, **arrow A**). The first 1 week post-surgical echocardiogram is indicated by **arrow B**. At 8 weeks post-surgery **(arrow C)**, the MI and Sham groups were randomly assigned to receive 60 to 80 μl of either rAAV9-GFP (3.1×10^{12} genome copies [GC]/ml; Sham- or MI-GFP) or rAAV9-BAG3 (5 to 6.5×10^{13} GC/ml; Sham- or MI-BAG3) by injection into the retro-orbital venous plexus. Serial echocardiography was performed to determine the ejection fraction (EF), including 1 week before and 9 days and 3 weeks **(arrow D)** after injection. Data was analyzed using a 2-way analysis of variance for repeated measures. n = 14 Sham-GFP, n = 12 Sham-BAG3, n = 12 MI-GFP, and n = 13 MI-BAG3. *MI-GFP versus -BAG3 at week 9, $p < 0.0001$; †MI-GFP versus -BAG3 at week 11, $p < 0.0001$. There was no statistical difference between Sham-GFP and -BAG3 at any time points. **(C)** Western blot analysis of BAG3 levels in right ventricles of MI-GFP, MI-BAG3, and Sham-GFP mice (n = 3) sacrificed 11 weeks post-MI (3 weeks post-injection of rAAV9-BAG3 or -GFP) *$p < 0.04$; MI-GFP compared with MI-BAG3 or Sham-GFP. Confocal images demonstrating normal BAG3 levels in Sham-GFP hearts **(D)** reduced BAG3 levels in MI-GFP myocytes **(E)** and reconstitution and correct targeting of exogenous BAG3 in MI-BAG3 myocytes **(F)**.

MEASUREMENT OF $[Ca^{2+}]_i$ AND CONTRACTION IN CARDIAC MYOCYTES. GFP-expressing myocytes were fura-2 loaded (0.67 μmol/l fura-2 AM, 15 min), incubated in 4-(2-hydroxyethyl)-1-piperazine ethanesulfonic acid-buffered (20 mmol/l, pH 7.4) medium 199 (1.8 mmol/l $[Ca^{2+}]_o$), and field stimulated to contract (2 Hz; 37°C), as described previously (9). In brief, myocytes were exposed to excitation light (360 and 380 nm) only during data acquisition. Epifluorescence (510 nm) was measured in steady-state twitches both before and after the addition of isoproterenol (1 μmol/l) (15–20). For contraction measurements, images of myocytes (not loaded with fura-2) were captured by a charge-coupled device video camera, and myocyte motion was analyzed offline with an edge detection algorithm (15–20).

CONFOCAL MICROSCOPY. Confocal microscopy was used to detect BAG3 localization in adult cardiomyocytes as described previously (9). Briefly, adult mouse LV cardiomyocytes were isolated and plated on laminin-coated 4-well chamber slides (Lab-Tek, Rochester, New York). BAG3 was identified using a primary rabbit antibody (1:200; ProteinTech Group Inc.). After incubation for 12 h at 20°C, myocytes were rinsed with PBS and then incubated with secondary Alexfluor 594-labeled goat anti-rabbit antibodies (1:500 Invitrogen, Eugene, Oregon) at rt in the dark

for 60 min. A Carl Zeiss 710 confocal microscope (63× oil objective) with ZEN software was used for imaging. Total laser intensity and photomultiplier gain were set constant for all groups and settings, and data were verified by 2 independent observers who were blinded to the experimental group. Three coverslips were used for each experimental group and at least 3 cell images were acquired from each coverslip.

REAL-TIME POLYMERASE CHAIN REACTION MEASUREMENT OF BRAIN NATRIURETIC PEPTIDE. Total messenger ribonucleic acid (mRNA) was isolated from a randomly selected group of sham or MI mice as described previously, with the exception of the use of a MirVana miRNA isolation kit (Thermo Fisher Scientific, Waltham, Massachusetts). Reverse-transcribed cDNA from 1 μg mRNA was used to determine the expression of B-type natriuretic peptide (BNP) from MI-GFP (6) and -BAG3 (5) mice as described previously (16). BNP primers were 5′ CTG AAG GTG CTG TCC CAG AT 3′ and 5′′ CCT TGG TCC TTC AAG AGC TG 3′, and GAPDH primers were 5′ AAC GAC CCC TTC ATT GAC 3′ and 5′ TCC ACG ACA TAC TCA GCA C 3′. GAPDH was used as a reference for normalization of BNP measurements. The ΔCT method was used to quantify the results. BNP expression was presented as a relative to the GAPDH gene.

STATISTICAL ANALYSIS. Data was analyzed using GraphPad Prism 6 (La Jolla, California) or JMP version 12 (SAS Institute, Cary, North Carolina). Data are presented as means ± SEM for continuous variables. Our experience with echocardiographic measurements in test animals and measures of Ca^{2+} homeostasis and contractility in cells has shown that the underlying distribution is normal. Furthermore, analysis of variance (ANOVA) is robust to moderate variations from normalcy. Therefore, we used 2-way ANOVA for repeated measures to assess the significance of the different groups, time, and the first-order interaction between group and time for echocardiographic measures. For analysis of the single-cell data in which cells were exposed to isoproterenol, we first analyzed the data for all 3 groups (Sham-GFP, MI-GFP, and MI-BAG3) together to make sure that statistical significance existed amongst the 3 groups and then considered group, isoproterenol, and first-order interaction between group and isoproterenol using 2-way ANOVA with Bonferroni multiple comparisons adjustments. A p value ≤0.05 was considered statistically significant.

RESULTS

rAAV9-BAG3 IMPROVES LV DYSFUNCTION IN MICE POST-MI. Preliminary studies demonstrated that myc-tagged rAAV9-BAG3 was appreciated by day 7 after retro-orbital injection and reached maximal levels of expression by day 9. (Figure 1A) Therefore, to assess the effects of increased expression of BAG3 on LV function post-MI, mice in both the Sham and MI groups were randomized within group just prior to the week-1 echocardiogram to receive either myc^{-}-tagged rAAV9-BAG3 (Sham- and MI-BAG3) or rAAV9-GFP (Sham- and MI-GFP) followed by sacrifice 3 weeks later. As shown in Figure 1B, compared with Sham-GFP mice, MI-GFP mice demonstrated a significant decrease in LVEF at 1 week post-MI with a progressive diminution in contractility over time. By contrast, compared with MI-GFP mice, MI-BAG3 mice demonstrated significantly ($p < 0.0001$) higher LVEF at 9 days post-rAAV9-BAG3 injection, and LVEF continued to improve at 3 weeks post-injection ($p < 0.0001$) (Table 1). Similarly, at 3 weeks post-injection, rAAV9-BAG3 resulted in a significant increase in stroke volume ($p < 0.0001$), FS ($p < 0.0001$), and LV posterior wall thickness in diastole ($p < 0.025$) in MI-BAG3 mice when compared with MI-GFP mice. However, injection of rAAV9-BAG3 did not affect LV mass, LV volume, or LV internal diameter in MI-BAG3 mice when compared with measurements in MI-GFP mice (Table 1). Importantly, injection of rAAV9-BAG3 had no effect on LVEF in Sham mice when compared with Sham mice that received rAAV9-GFP. It is also noteworthy that there was no statistical difference in LVEF between MI-BAG3 and -GFP mice at weeks 1, 3, 5, or 7—all of which were prior to the injection of rAAV9-BAG3 or -GFP at week 8. Preliminary studies had demonstrated that the fall in ejection fraction post-MI in our model plateaued

TABLE 1 Cardiac Function Measured By Echocardiography

Measurement	Sham-GFP (14)	Sham-BAG3 (12)	MI-GFP (10)	MI-BAG3 (10)
LVIDd, mm	3.93 ± 0.08	4.16 ± 0.08	4.74 ± 0.19*†	4.88 ± 0.13‡
LVIDs, mm	2.54 ± 0.11	2.83 ± 0.06	3.98 ± 0.21†§	3.43 ± 0.18‖
LVPWd, mm	1.03 ± 0.08	0.86 ± 0.03	1.58 ± 0.14†§	1.11 ± 0.08¶
LVPWs, mm	1.37 ± 0.06	1.10 ± 0.04	1.71 ± 0.16§	1.43 ± 0.07
EF, %	68.83 ± 0.97	65.86 ± 1.21	34.9 ± 2.29†§	58.85 ± 1.31#
FS, %	35.61 ± 1.94	32.05 ± 1.17	15.85 ± 1.59*†	30.04 ± 2.35#
LVVold, ml	67.85 ± 3.54	77.99 ± 3.52	105.7 ± 9.96†§	115.3 ± 8.39‡#
LVVols, ml	24.64 ± 2.56	31.14 ± 1.66	72.26 ± 9.26†§	51.33 ± 6.6
LV mass, mg	134.8 ± 13.9	125.3 ± 11.46	229.1 ± 21.0*†	229.4 ± 25.78‡
SV, ml	43.19 ± 2.16	46.93 ± 2.87	33.45 ± 3.32*	63.93 ± 5.04‡#

Values are mean ± SEM. *$p < 0.025$ compared with Sham-BAG3. †$p < 0.001$ compared with Sham-GFP. ‡$p < 0.01$ compared with Sham-BAG3. §$p < 0.0001$ compared with Sham-BAG3. ‖$p < 0.025$ compared with Sham-BAG3. ¶$p < 0.025$ compared with MI-GFP. #$p < 0.0001$ compared with MI-GFP.

BAG3 = Bcl-2-associated athanogene 3; EF = ejection fraction; FS = fractional shortening; GFP = green fluorescent protein; LV = left ventricular; LVIDd = left ventricular internal diameter, diastole; LVIDs = left ventricular internal diameter, systole; LVPWd = left ventricular posterior wall thickness in diastole; LVPWs = left ventricular posterior wall thickness in systole; LVVold = left ventricular volume, diastole; LVVols = left ventricular volume, systole; MI = myocardial infarction; rAAV9 = adeno-associated virus serotype 9; SV = stroke volume.

FIGURE 2 BAG3 Overexpression Improves Myocyte Contractility Post-MI

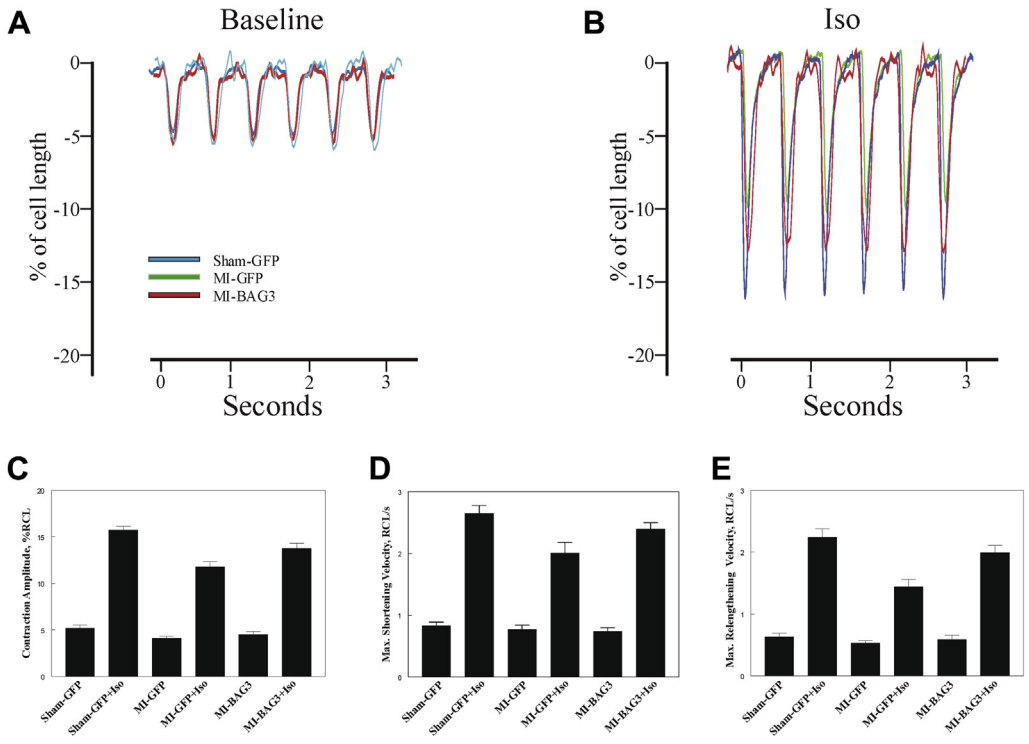

Myocytes were isolated from the left ventricles and septum of the 3 groups of mice (n = 3 mice each) used in Figure 1, with care being taken to excise the infarct scar in MI-GFP and -BAG3 hearts. In Sham-GFP hearts, the area corresponding to the infarct scar in MI hearts was excised before myocyte isolation. Representative contraction traces obtained in freshly isolated myocytes (2 Hz, 37°C, 1.8 mmol/l $[Ca^{2+}]_o$) (please see the Methods section) are shown at baseline **(A)** and after 1 μmol/l of isoproterenol (Iso) **(B)**. Contraction amplitudes **(C),** maximal shortening **(D)**, and re-lengthening velocities **(E)** are shown for Sham-GFP, MI-GFP, and MI-BAG3 myocytes, both at baseline and in the presence of isoproterenol. There are 17 Sham-GFP, 18 MI-GFP, and 25 MI-BAG3 myocytes at baseline and 21 Sham-GFP, 18 MI-GFP, and 17 MI-BAG3 myocytes after isoproterenol. Differences between groups are analyzed with 2-way analysis of variance are given in the Results section. RCL = resting call length; other abbreviations as in Figure 1.

between weeks 5 and 7. Therefore, we chose to inject AAV9-BAG3 at week 8, a time when the EF was relatively stable, to optimize our ability to assess the effects of rAAV9-BAG3. Also, it should be noted that there were no deaths in mice randomized to any of the 4 treatment groups after injection of either rAAV9-BAG3 or -GFP.

As we have previously observed in other models of HF (1), levels of BAG3 were significantly diminished in MI-GFP mice at 11 weeks post-MI compared with Sham-GFP mice ($p < 0.04$); however, MI-BAG3 mice had significantly elevated levels of BAG3 compared with MI-GFP mice ($p < 0.04$) (Figure 1C). Consistent with earlier findings in our laboratory (9), BAG3 was found predominantly in the sarcolemma and t-tubules of Sham-GFP myocytes. BAG3 levels were reduced in MI-GFP myocytes. Importantly, not only did rAAV9-BAG3 injection reconstitute BAG3 levels, but the exogenous BAG3 was also correctly targeted to the sarcolemma and t-tubules of MI-BAG3 myocytes (Figures 1D to 1F). We did not measure BNP levels as part of our original protocol; however, we were able to assess levels of BNP in a subgroup of MI-BAG3 and -GFP hearts. There was a trend toward a decrease in BNP mRNA levels in the hearts of MI mice that received rAAV9-BAG3 (4.87 ± 0.52; n = 5; presented as relative to GAPDH expression) as compared with those that received rAAV9-GFP (2.96 ± 0.71; n = 6); however, the difference did not meet statistical significance ($p = 0.670$).

EFFECTS OF AAV9-BAG3 ON INDIVIDUAL MYOCYTES POST-MI. To confirm the salutary in vivo effects of rAAV9-BAG3 on myocardial contractility in mice that had undergone an MI and to dissect the physiological effects of gene therapy, we assessed the effect of rAAV9-BAG3 expression on individual myocytes isolated from a randomly selected cohort of MI-BAG3,

FIGURE 3 BAG3 Overexpression Improves $[Ca^{2+}]_i$ Dynamics Post-MI

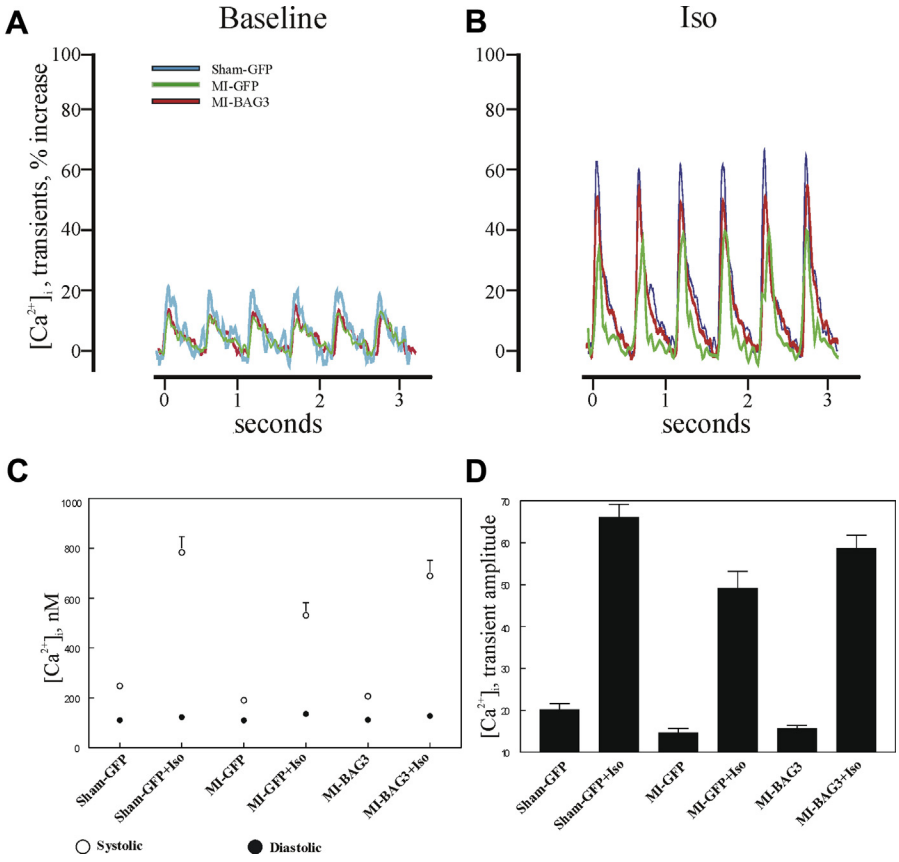

$[Ca^{2+}]_i$ transients were measured in fura-2 loaded myocytes (2 Hz, 37°C, 1.8 mmol/l $[Ca^{2+}]_o$) and representative traces are shown both at baseline **(A)** and after isoproterenol (1 μmol/l) **(B)**. Summaries of systolic and diastolic $[Ca^{2+}]_i$ **(C)** and $[Ca^{2+}]_i$ transient amplitudes **(D)** are shown. **Error bars** are not shown if they fall within the boundaries of the **symbols**. There are 15 Sham-GFP, 16 MI-GFP, and 21 MI-BAG3 myocytes at baseline, and 11 Sham-GFP, 13 MI-GFP, and 18 MI-BAG3 myocytes after isoproterenol. Differences between groups are analyzed with 2-way analysis of variance and are given in the Results section. There are no differences in $[Ca^{2+}]_i$ transients between Sham-GFP and MI-BAG3 myocytes. Abbreviations as in Figure 1.

MI-GFP, and Sham-GFP hearts 11 weeks post-MI (3 weeks post-AAV9-BAG3 injection). Compared with Sham-GFP myocytes, contraction amplitudes in MI-GFP myocytes were significantly lower at baseline, and the differences were amplified in the presence of isoproterenol (Figures 2A to 2C) (Sham- vs. MI-GFP; $p = 0.0004$; group × iso interaction effect). BAG3 overexpression improved contractility in post-MI myocytes toward normal: the beneficial effect was more prominent in the presence of isoproterenol (MI-GFP vs. -BAG3; $p = 0.054$; group × iso interaction effect). Compared with Sham-GFP myocytes, maximal shortening (Figure 2D) ($p = 0.0162$) and relengthening (Figure 2E) ($p = 0.001$) velocities were depressed in MI-GFP myocytes. Overexpression of BAG3 improved isoproterenol-stimulated cell shortening (MI-BAG3 vs. -GFP; $p = 0.046$) and relengthening (MI-BAG3 vs. -GFP; $p = 0.012$) velocities post-MI.

EFFECTS OF BAG3 OVEREXPRESSION ON $[Ca^{2+}]_i$ TRANSIENTS POST-MI. Ca^{2+} occupies a central role in excitation-contracting coupling, and alterations in $[Ca^{2+}]_i$ dynamics may account for the contractility differences observed among the 3 groups of myocytes. Compared to Sham-GFP myocytes, systolic $[Ca^{2+}]_i$ was significantly lower in MI-GFP myocytes ($p = 0.009$; group × iso interaction effect) (Figures 3A to 3C). BAG3 overexpression restored systolic $[Ca^{2+}]_i$ in post-MI myocytes toward that observed in Sham-GFP myocytes (Figure 3C) (Sham-GFP vs. MI-BAG3; $p = 0.504$; group × iso interaction effect). Diastolic $[Ca^{2+}]_i$ was not different among the 3 groups ($p = 0.722$; group × iso interaction effect) (Figure 3C). Compared with

FIGURE 4 BAG3 Overexpression Increases Peak I_{Ca} Amplitudes Post-MI

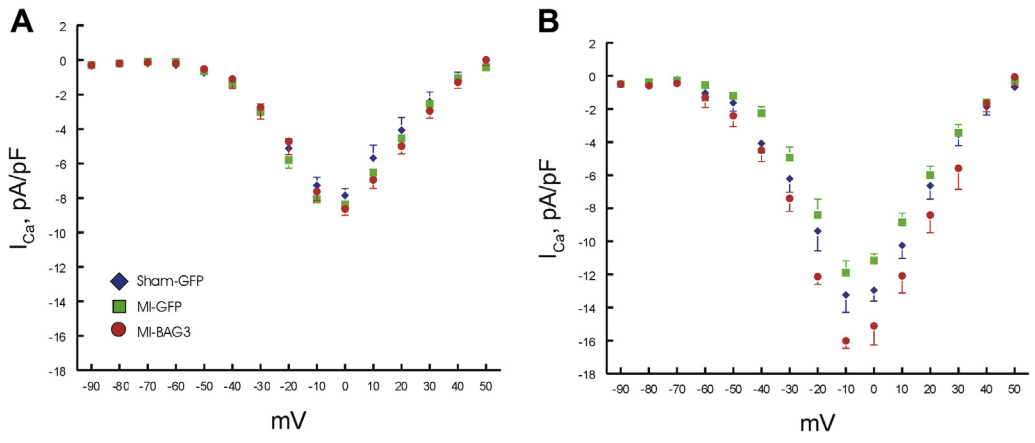

L-type Ca^{2+} current (I_{Ca}) ($[Ca^{2+}]_o$ 2 mmol/l) in 8 Sham-GFP, 8 MI-GFP, and 6 MI-BAG3 myocytes (3 mice each group) are measured at baseline **(A)** and after 1 μmol/l isoproterenol **(B). Error bars** are not shown if they fall within the boundaries of the **symbols**. Abbreviations as in **Figure 1**.

Sham-GFP myocytes, $[Ca^{2+}]_i$ transient amplitudes were significantly reduced in MI-GFP myocytes (**Figure 3D**) ($p = 0.026$; group × iso interaction effect). In addition, rAAV9-BAG3 increased $[Ca^{2+}]_i$ transient amplitudes in post-MI myocytes toward levels observed in Sham-GFP myocytes (Sham-GFP vs. MI-BAG3; $p = 0.518$, group × iso interaction effect) (**Figure 3D**).

EFFECTS OF BAG3 OVEREXPRESSION IN L-TYPE Ca^{2+} CURRENT POST-MI. L-type Ca^{2+} current (I_{Ca}), the physiological trigger for sarcoplasmic reticulum (SR) Ca^{2+} release, is a major determinant of $[Ca^{2+}]_i$ transient amplitude. Our observation that $[Ca^{2+}]_i$ transient amplitudes differed among the 3 groups of myocytes prompted us to measure I_{Ca}. At baseline, maximal I_{Ca} amplitudes and voltage at which I_{Ca} peaked were similar among Sham-GFP, MI-GFP, and MI-BAG3 myocytes ($p = 0.042$) (**Figure 4A**). In the presence of isoproterenol, maximal I_{Ca} amplitude tended to be lower ($p = 0.081$) in MI-GFP when compared with Sham-GFP myocytes (**Figure 4B**). Treatment with rAAV9-BAG3 increased maximal I_{Ca} amplitude post-MI to levels that were even higher ($p = 0.042$) than those measured in Sham-GFP myocytes (**Figure 4B**).

DISCUSSION

In this proof-of-concept study, we demonstrate for the first time that delivery of BAG3 to the heart using rAAV9 and murine *BAG3* under the control of the CMV promoter significantly increased LV function in mice with substantially diminished LV function secondary to an MI. BAG3 has pleiotropic effects in cells due to the presence of multiple protein binding motifs. For example, it binds to the ATPase domain of heat shock protein-70 to effect protein quality control (21), interacts with Bcl-2 to impart an antiapoptosis function, and regulates a diverse portfolio of cellular processes including development, cytoskeletal arrangement, and mitophagy (2). Our observation that BAG3 couples the β1AR and the L-type Ca^{2+} channel within the sarcolemma of adult cardiac myocytes and the finding that rAAV9-BAG3 increases LV performance in hearts with diminished LV function after an MI are consistent with this pleiotropism (9).

Studies in mice harboring a homozygous deletion of BAG3 that develop myofibrillar degeneration and death by 4 weeks of age (7), observations in children with a point mutation (p.Pro209Leu) in BAG3 who have a dystrophin-like phenotype and cardiac hypertrophy (3–6,22,23), diminished levels of BAG3 in failing human hearts and in animal models of HF (1), the observation that the myofibrillar structure of neonatal myocytes is disrupted after BAG3 is knocked down (8), and our observation that BAG3 facilitates the ability of β-adrenergic signaling to augment cardiac contraction through linkage of the β1AR and the L-type Ca^{2+} channel and subsequent alterations in Ca^{2+} homeostasis suggest that BAG3 plays an important role in cardiac homeostasis (9). Our findings that rAAV9-BAG3 correctly targeted the exogenous BAG3 to the sarcolemma and t-tubules and improved LV function in mice after an MI is consistent with these earlier studies. Furthermore, we confirmed our in vivo findings in individual myocytes that were isolated from MI-BAG3, MI-GFP, and Sham-GFP mice.

Intuitively, an increase in contractility due to enhanced Ca^{2+} homeostasis might presage an increased risk for arrhythmogenesis. However, several lines of reasoning suggest that this is not the case: 1) diastolic Ca^{2+} was not different between MI-GFP and -BAG3 myocytes in the presence of isoproterenol, suggesting that the cells were not Ca^{2+} overloaded; 2) the lower I_{Ca} in post-MI myocytes compared with Sham myocytes in the presence of isoproterenol was attributable to βAR uncoupling and not to alterations in ion channel function, because forskolin or dibutyryl cyclic adenosine monophosphate restored I_{Ca} to normal (24); and 3) there were no deaths in any of the experimental groups after injection of rAAV9. Thus, there does not appear to be a cellular substrate for arrhythmias, although longer follow-up post-rAAV9-BAG3 will be required to completely eliminate this possibility.

STUDY LIMITATIONS. This proof-of-concept study was focused on evaluating the early effects of increasing BAG3 expression in the heart in vivo using an adeno-associated virus under the control of a CMV promoter. As a result, we were not able to detect the potential effects of BAG3 on cardiac remodeling. For example, the salutary effects of rAAV9-BAG3 on LV function were not associated with a change in LV mass or size. However, we did see a trend toward a decrease in BNP levels in MI-BAG3 hearts when compared with MI-GFP hearts in an evaluation of a subset of the overall study group.

CONCLUSIONS

The consistent observation that rAAV9-BAG3 had no untoward effect on ventricular function in Sham-BAG3 mice when compared with Sham-GFP mice has important implications for the potential use of rAAV9-BAG3 as a novel treatment strategy, because it suggests that after a finite level of cellular BAG3 is reached, subsequent protein expression does not have deleterious effects. Because inotropic responses do not necessarily guarantee clinical responses, it will be important to evaluate the long-term effects of BAG3 overexpression on contractile function and on cellular processes that play a role in cell survival, including apoptosis and autophagy. Nonetheless, the results of this proof-of-concept study suggest that BAG3 may be a novel and potentially effective therapeutic target in patients with loss of function biallelic mutations and in those with nonfamilial dilated cardiomyopathy, and that further investigations to clarify the effects of rAAV9-BAG3 and its mechanisms of action in the heart are warranted.

ACKNOWLEDGMENT The results are part of the doctoral thesis of Dr. Knezevic.

REPRINT REQUESTS AND CORRESPONDENCE: Dr. Arthur M. Feldman, Department of Medicine, Lewis Katz School of Medicine at Temple University, 3401 North Broad Street, Suite C902 Parkinson Pavilion, Philadelphia, Pennsylvania 19106. E-mail: Arthur.Feldman@tuhs.temple.edu.

PERSPECTIVES

COMPETENCY IN MEDICAL KNOWLEDGE: It is becoming increasingly evident that a substantial proportion of idiopathic dilated cardiomyopathy is due to genetic variants and that these variants are often passed down among family members in an autosomal dominant fashion. Although recognition of familial forms of heart failure has not yet led to specific treatments, identification of large families with heritable forms of the disease can lead to the discovery of new therapeutic targets, thus reinforcing the importance of the family history in the workup of a patient with new onset heart failure.

TRANSLATIONAL OUTLOOK: Although the present study demonstrates proof of concept that re-expression of BAG3 can improve LV function in mice after an MI, several steps will be required before these findings can be translated into man, including evaluation of the long-term effects of BAG3 expression and proof of concept in a large animal model.

REFERENCES

1. Knezevic T, Myers VD, Gordon J, et al. BAG3: a new player in the heart failure paradigm. Heart Fail Rev 2015;20:423–34.

2. Behl C. Breaking BAG: the co-chaperone BAG3 in health and disease. Trends Pharmacol Sci 2016;37:672–8.

3. Odgerel Z, Sarkozy A, Lee HS, et al. Inheritance patterns and phenotypic features of myofibrillar myopathy associated with a BAG3 mutation. Neuromuscul Disord 2010;20:438–42.

4. Selcen D, Muntoni F, Burton BK, et al. Mutation in BAG3 causes severe dominant childhood muscular dystrophy. Ann Neurol 2009;65:83–9.

5. Feldman AM, Begay RL, Knezevic T, et al. Decreased levels of BAG3 in a family with a rare variant and in idiopathic dilated cardiomyopathy. J Cell Physiol 2014;229:1697–702.

6. Norton N, Li D, Rieder MJ, et al. Genome-wide studies of copy number variation and exome sequencing identify rare variants in BAG3 as a cause of dilated cardiomyopathy. Am J Hum Genet 2011;88:273–82.

7. Homma S, Iwasaki M, Shelton GD, Engvall E, Reed JC, Takayama S. BAG3 deficiency results in fulminant myopathy and early lethality. Am J Pathol 2006;169:761–73.

8. Hishiya A, Kitazawa T, Takayama S. BAG3 and Hsc70 interact with actin capping protein CapZ to maintain myofibrillar integrity under mechanical stress. Circ Res 2010;107:1220–31.

9. Feldman AM, Gordon J, Wang J, et al. BAG3 regulates contractility and Ca^{2+} homeostasis in adult mouse ventricular myocytes. J Mol Cell Cardiol 2016;92:10–20.

10. Gao E, Lei YH, Shang X, et al. A novel and efficient model of coronary artery ligation and myocardial infarction in the mouse. Circ Res 2010; 107:1445–53.

11. Most P, Seifert H, Gao E, et al. Cardiac S100A1 protein levels determine contractile performance and propensity toward heart failure after myocardial infarction. Circulation 2006;114:1258–68.

12. Tilley DG, Zhu W, Myers VD, et al. β-adrenergic receptor-mediated cardiac contractility is inhibited via vasopressin type 1A-receptor-dependent signaling. Circulation 2014;130:1800–11.

13. Yardeni T, Eckhaus M, Morris HD, Huizing M, Hoogstraten-Miller S. Retro-orbital injections in mice. Lab Anim (NY) 2011;40:155–60.

14. Zhou YY, Wang SQ, Zhu WZ, et al. Culture and adenoviral infection of adult mouse cardiac myocytes: methods for cellular genetic physiology. Am J Physiol Heart Circ Physiol 2000;279: H429–36.

15. Tucker AL, Song J, Zhang XQ, et al. Altered contractility and $[Ca^{2+}]_i$ homeostasis in phospholemman-deficient murine myocytes: role of Na^+/Ca^{2+} exchange. Am J Physiol Heart Circ Physiol 2006;291:H2199–209.

16. Song J, Gao E, Wang J, et al. Constitutive overexpression of phosphomimetic phospholemman S68E mutant results in arrhythmias, early mortality, and heart failure: potential involvement of Na^+/Ca^{2+} exchanger. Am J Physiol Heart Circ Physiol 2012;302:H770–81.

17. Song J, Zhang XQ, Wang J, et al. Regulation of cardiac myocyte contractility by phospholemman: Na^+/Ca^{2+} exchange versus Na^+ -K^+ -ATPase. Am J Physiol Heart Circ Physiol 2008; 295:H1615–25.

18. Wang J, Chan TO, Zhang XQ, et al. Induced overexpression of Na^+/Ca^{2+} exchanger transgene: altered myocyte contractility, $[Ca^{2+}]_i$ transients, SR Ca^{2+} contents, and action potential duration. Am J Physiol Heart Circ Physiol 2009;297: H590–601.

19. Wang J, Gao E, Rabinowitz J, et al. Regulation of in vivo cardiac contractility by phospholemman: role of Na^+/Ca^{2+} exchange. Am J Physiol Heart Circ Physiol 2011;300:H859–68.

20. Wang J, Gao E, Song J, et al. Phospholemman and β-adrenergic stimulation in the heart. Am J Physiol Heart Circ Physiol 2010;298:H807–15.

21. Takayama S, Xie Z, Reed JC. An evolutionarily conserved family of Hsp70/Hsc70 molecular chaperone regulators. J Biol Chem 1999;274: 781–6.

22. Lee HC, Cherk SW, Chan SK, et al. BAG3-related myofibrillar myopathy in a Chinese family. Clin Genet 2012;81:394–8.

23. Villard E, Perret C, Gary F, et al. A genome-wide association study identifies two loci associated with heart failure due to dilated cardiomyopathy. Eur Heart J 2011;32:1065–76.

24. Zhang XQ, Moore RL, Tillotson DL, Cheung JY. Calcium currents in postinfarction rat cardiac myocytes. Am J Physiol 1995;269:C1464–73.

KEY WORDS BAG3, gene therapy, heart failure, left ventricular function, myocardial infarction